Nada F. Mahdi
Mithaq M.M. Al-Sultani

Department of Physics,
College of Education for Girls,
University of Kufa,
Najaf, IRAQ

Thermal Properties of Fragmented Human Kidney Stones by Ho:YAG Laser

This study aims at investigating the thermal properties of various kidney stone types that fragmented by laser. It attempts to understand their behavior during Ho:YAG laser with maximum power of 30 W. The pulse duration is 600 μs, wavelengths is 2100 nm, and the maximum energy level is 5J with maximum frequency level 30Hz. This is used for lithotripsy in Al-Sadr Medical City in Najaf for 40 samples divided to 27 calcium oxalate, 11 uric acid, 1 cystine, and 1 protein. Optical penetration depth, thermal diffusion time, temperature rise, and thermal relaxation time have been calculated using established equations. The Optical penetration depth is varied between 0.165-0.327 mm, the highest value has been recorded in sample p12. The highest temperature levels are observed in calcium oxalate sample P5 and uric acid sample P14. Temperature rise increases with increasing pulse energy in both calcium oxalate and uric acid stones.

Keywords: Ho:YAG laser; Calcium oxalate; Uric acid; Kidney stones
Received: 13 January 2024; **Revised:** 15 February 2024; **Accepted:** 22 February 2024

1. Introduction

Urinary stone disease is still a major problem throughout the world, and kidney stones are one of the most common and painful ailments of the urinary system [1]. Known also as uroliths or the kidney/ureter/bladder/urethra calculus, urinary calculi are crystalline deposits that develop in the urinary system [2]. Kidney stone disease affects 50 million persons worldwide and 10% of Americans [3]. It is noted that the ailment is becoming more common; during the course of their lives, 7% of women and 12% of men will be affected [4]. Urinary tract stones are classified into various categories based on the materials or crystals that make them up [1]. Calcium stones are the most prevalent kind of renal stones, accounting for around 80% of all urinary calculi [5]. Most kidney stones are composed totally or partially of CaOx, which can occur as a monohydrate (COM) or dihydrate (COD) [6-8]. Eight to ten percent of kidney stones worldwide are uric acid stones, which are disproportionately common in obese and insulin-resistant stone formers—two major markers of metabolic syndrome. Unlike calcium stone types, urine with a pH of less than 5.5 is the primary source of uric acid nephrolithiasis. [5,7]. While other forms of kidney stones do exist, they are less common than uric acid and calcium stones [9,10]. Over the past ten years, advancements in the three primary components of laser lithotripsy—optical fiber, ureteroscope, and laser—have made the operation more widely used in clinical settings. For nearly two decades, the gold standard for lithotripsy has been the Holmium:YAG infrared laser, which is powered by a flashlamp and has a long pulse duration [11-13]. The Ho:YAG laser's architecture shifts depending on the power supply used to pump the crystal. Flashlamp light (usually Xenon or Krypton) is used to create laser pulses, and when it interacts with the Holmium ions, it causes them to generate new photons at a wavelength of 2120 nm [14,15]. The delivery of holmium laser energy occurs via a compact optical fiber, resulting in the fragmentation of the stone into numerous smaller pieces [4,16]. These fragments can then be extracted individually using a stone basket. Alternatively, if the stone size is reduced to 2 mm or smaller, it can traverse the urinary tract without obstruction and be naturally expelled by the patient [17]. The tiny, malleable optical fibers with diameters between 200 and 1000 μm are used [18]. Because of its adaptability, lithotripsy may be performed anywhere in the upper urinary system, including during flexible ureteroscopy (FURS) and flexible nephroscopy [12,19,20]. The photothermal effect is the first stage of interaction the laser light with tissue. Tissue can be rapidly heated with a laser by absorb some of the light, and then their vibrations and collisions transform some of that energy into heat. The laser's adjustable settings allow for a range of thermal effects on tissue. These include coagulation, evaporation, and selective thermolysis (heat-induced chemical/cell disintegration) [21,22].

2. Materials and Methods

Forty samples that have been collected from Al-Sader Medical City in the city of Najaf as shown in Fig. (1), were fragmented by Ho:YAG laser with a maximum power of 30 W, pulse duration of 600 μs, wavelengths 2100 nm, the maximum energy level 5J with maximum frequency level 30Hz. This laser from Litho company and brand Quanta System Italy with optical fiber from the REOSABLE company have been used with a diameter of 550 µm to insert the laser beams into the ureter and shine the rays on the stones. The patient is positioned on an exam table and the urethra is numbed with a local anesthetic. The laser is passed by the optical fiber through a thin tube (catheter) that is inserted into the ureter through the urethra. The laser fragments the stone into small pieces less than 4 mm that can be passed out of the body in the urine. A stone sample was taken from

each patient, its chemical and optical properties were studied by FTIR-ATR analyzer, and the value of the optical absorption coefficient was calculated.

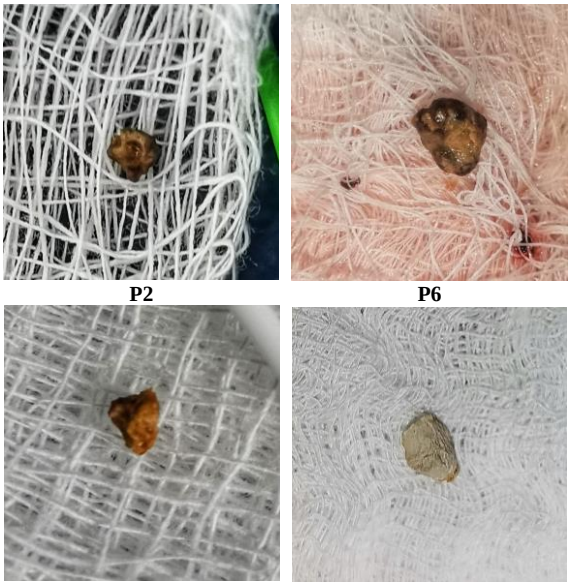

Fig. (1) Pictures of different samples

3. Results and Discussion

The results of the FTIR-ATR analyzer show that the majority of the stone samples have been of the calcium oxalate type, labeled 27, 11 of the acid type stones, one sample of cystine, and one sample of protein. Each stone sample is not completely pure, but contains different proportions of other types of other substances, such as uric acid, ammonium urate, sodium urate, and carbonate apatite. But they can be considered one species according to the proportion of its predominant substance. The optical penetration depth δ for the highest absorption coefficient ($\mu_a(\lambda)$) for every stone is calculated by using [23]:

$$\delta = \frac{1}{\mu_a(\lambda)} \quad (1)$$

As noticed in table (1), although it is the same type as in samples P1, P6, P7, P12, and P21, the absorption coefficient differs from one stone to another. This is due to the difference in absorbance and may be due to the presence of other percentages of different types of substances in the stones. What confirms this result is that the ratios in the P6 and P7 samples are the same. So, it can be found that the absorbance is the same and the results are all the same. This applies to all other samples. It is, also, noted in table (1) that the highest value of penetration depth is in sample P12 due to its low absorbance, as the penetration depth ranges between 0.165- 0.327 mm. These results agree with the results of researches [24-26].

The thermal diffusion time (τ_{TH}), the temperature rise ($\Delta T(\chi)$) and thermal relaxation time (t_{st}) are calculated by equations (2), (3) and (4), respectively.

$$\tau_{TH} = \frac{\delta^2}{4\alpha} \quad (2)$$

where α represent the thermal diffusivity (i.e., α = 0.15 mm^2/sec for water at 37°C) [23].

$$\Delta T(\chi) = \frac{\mu_a(\lambda) H_o}{\rho c_p} e^{-\mu_a(\lambda)\chi} \quad (3)$$

where ΔT represents differential temperature increase, ρ represents the material density, the densities of COM and COD are 2.17 and 1.96 g/cm^3, respectively [27]. c_p represents the material specific heat at constant pressure for calculus is about 1524 J/kg.°C [28], H_o represents the surface fluence, and χ is depth [23].

$$t_{st} = \frac{\delta}{c} \quad (4)$$

Here c is the speed of sound [29].

Figure (2) shows the highest temperature rise in P5 sample for calcium oxalate stones, while in Fig. (3), sample P14 has the highest temperature rise for uric acid stones due to high energy pulse used in fragmentation and high $\mu_a(\lambda)$ of the sample compared to other samples.

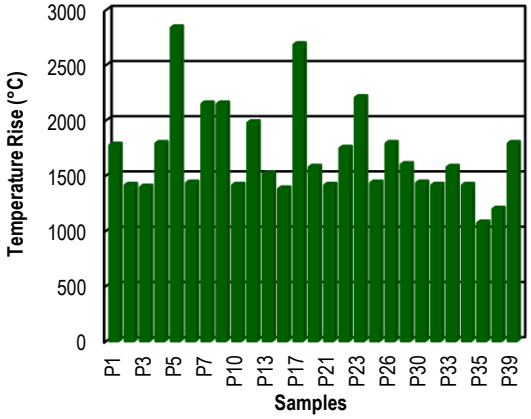

Fig. (2) The temperature rise for calcium oxalate stones

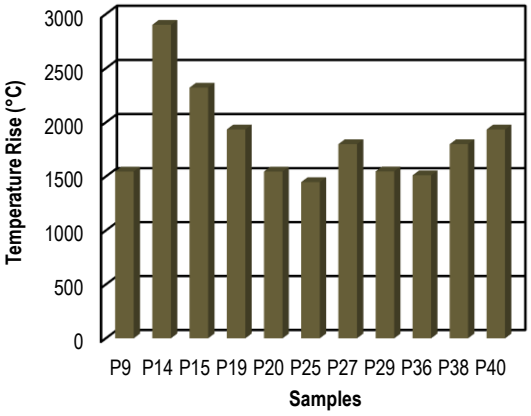

Fig. (3) The temperature rise for uric acid stones

Moreover, it is noticed that the temperature rise increases with increasing the energy of the pulse in both types of kidney stones, calcium oxalate and uric acid, as in figures (4) and (5). Where the high temperature values in the results are normal in the Ho:YAG laser, as this has been shown in different studies "Schafer and coworkers investigators reported a blackbody temperature of 5000°K from the irradiated calculus" [23,24]. It can be noticed that the

relaxation time is much less than the pulse duration, this indicates that the stones absorb the pulse energy during the pulse duration only and the heat dissipates quickly.

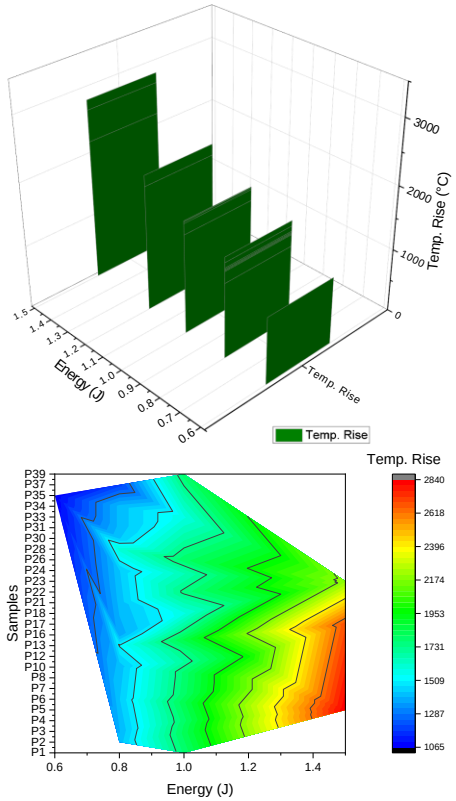

Fig. (4) The temperature rise for calcium oxalate stones with its energy pulse

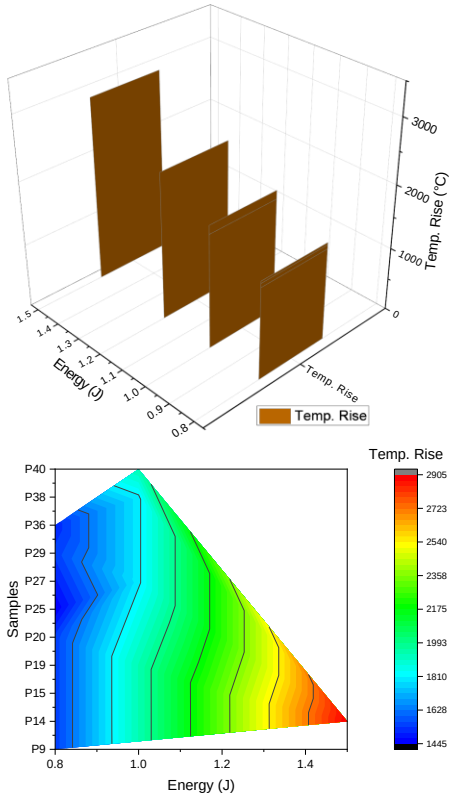

Fig. (5) The temperature rise for uric acid stones with its energy pulse

4. Conclusions

The key conclusion of the study is that kidney stone composition and optical properties have a significant impact on laser lithotripsy outcomes. The study identifies calcium oxalate as the predominant stone type (67.5%), followed by uric acid (27.5%), with rare occurrences of cystine and protein stones. The variation in absorption coefficient influence laser interaction even within the same stone type (e.g., P1-7, P12, P21). While penetration depth varies (0.165-0.327mm), temperature rise increases with pulse energy for both calcium oxalate and uric acid stones. Sample-specific properties like high absorption in P14 (uric acid) lead to the highest temperature increases about 2902.03°C. These findings underscore the importance of pre-operative stone characterization to determine composition and optical properties. By understanding the interplay between stone type, absorption coefficient, and penetration depth, laser settings can be customized to achieve optimal fragmentation with minimal collateral damage.

Acknowledgment

The authors offer their thanks and gratitude to Najaf health department for facilitating entry to the operating room of Al-Sadr Hospital in Najaf city to collect data. We also thank all the medical staff for their support and dedication to completing this study. We are very grateful for the Department of Physics, College of Education for Girls, University of Kufa, Iraq for allowing us to do this work. Also, we hope this research will be a reason to accomplish more future development.

References

[1] L.G. Awazli and A.S. Mahmood, "Urinary Tract Stones Fragmentation using 2100nm Ho:YAG Laser: *in vitro* Analysis", *Iraqi J. Laser*, 12 (2013) 1-12.
[2] J.J. Zhang et al., "Numerical Response Surfaces of Volume of Ablation and Retropulsion Amplitude by Settings of Ho:YAG Laser Lithotripter", *J. Healthcare Eng.*, 2018 (2018) 1-11.
[3] L.A. Hardy et al., "Fragmentation and Dusting of Large Kidney Stones using Compact, Air-cooled, High Peak Power, 1940-nm, Thulium Fiber Laser", *Therapeut. Diagnost. Urology*, 10468 (2018).
[4] D.S. Frank et al., "Polymer − Mineral Composites Mimic Human Kidney Stones in Laser Lithotripsy Experiments", *ACS Biomater Sci. Eng.*, 5(10) (2019) 4970-4975.
[5] T. Alelign and B. Petros, "Kidney Stone Disease : An Update on Current Concepts", *Adv. Urol.*, (2018) 1-12.
[6] S.R. Khan et al., "Kidney stones", *Nat. Rev. Dis. Primers*, 2(1) (2016) 1–23.
[7] O.W. Moe, "Kidney stones: pathophysiology and medical management", *The Lancet*, 367(9507) (2006) 333–344.

[8] F.L. Coe, A. Evan and E. Worcester, "Kidney stone disease", *J. Clin. Invest.*, 115(10) (2005) 2598–2608.
[9] M.E. Mayo, "Interaction of Laser Radiation with Urinary Calculi", Ph.D. thesis, Cranfield University (2009).
[10] E. Meimaridou, "Calcium Oxalate Modulation of Tubular Epithelial Cell Mitochondria: Oxidative Vulnerability Due to Restricted Glutathione Homeostasis", Ph.D. thesis, University College London (2007).
[11] D.E. Johnson, D.M. Cromeens and R.E. Price, "Use of the holmium: YAG laser in urology", *Lasers Surg. Med.*, 12(4) (1992) 353–363.
[12] E. Emiliani, "Evaluation of Ho:YAG Laser settings for the Non-Contact Stone Fragmentation Technique and the Curved Laser Fiber", Ph.D. thesis, (2019).
[13] A.D. Mahajan and S.A. Mahajan, "Thulium fiber laser versus Ho:YAG laser for stone lithotripsy during mini-percutaneous nephrolithotomy: A prospective randomized trial", *Indian J. Urol.*, 38(1) (2022) 1-42.
[14] P.T. Cleve, "Sur deux nouveaux éléments dans l'erbine", *CR. Acad. Sci.*, 89(9) (1879) 478–480.
[15] O. Traxer and E. X. Keller, "Thulium fiber laser: the new player for kidney stone treatment? A comparison with Ho:YAG laser", *World J. Urol.*, 38(8) (2020) 1883-1894.
[16] O. Schatloff et al., "Randomized Trial of Stone Fragment Active Retrieval versus Spontaneous Passage During Holmium Laser Lithotripsy for Ureteral Stones", *J. Urol.*, 183(3) (2010) 1031-1036.
[17] N.M. Fried, "Recent advances in infrared laser lithotripsy", *Biomed Opt. Exp.*, 9(9) (2018) 4552-4568.
[18] P. Kronenberg and O. Traxer, "The truth about laser fiber diameters", *Urology*, 84(6) (2014) 1301–1307.
[19] B.K. Somani et al., "Outcomes of Flexible Ureterorenoscopy and Laser Fragmentation for Renal Stones: Comparison between Digital and Conventional Ureteroscope", *Urology*, 82(5) (2013) 1017–1019.
[20] O.A. Nazif et al., "Review of Laser Fibers: A Practical Guide for Urologists", *J. Endourol.*, 18(9) (2004) 818–829.
[21] S. Thomse, "Pathologic Analysis of Photothermal and Photomechanical Effects of Laser-Tissue Interactions", *Photochem. Photobiol.*, 53(6) (1991) 825–835.
[22] M.H. Niemz, **"Laser-Tissue Interactions"**, Springer-Verlag Berlin Heidelberg (2007) p. 322.
[23] K.F. Chan et al., "A Perspective on Laser Lithotripsy: The Fragmentation Processes", *J. Endourol.*, 15(3) (2001).
[24] S.L. Jacques, "Laser-Tissue interactions: Photochemical, photothermal, and photomechanical", *Surg. Clin. North America*, 72(3) (1992) 531–558.
[25] R.S. Terry, P.S. Whelan and M.E. Lipkin, "New devices for kidney stone management", *Curr. Opin. Urol.*, 30(2) (2019) 144–148.
[26] G.M. Hale and M.R. Querry, "Optical Constants of Water in the 200-nm to 200-Mm Wavelength Region", *Appl. Opt.*, 12(3) (1973) 555–563.
[27] R.C. Walton, J.P. Kavanagh and B.R. Heywood, "The density and protein content of calcium oxalate crystals precipitated from human urine: a tool to investigate ultrastructure and the fractional volume occupied by organic matrix", *J. Struct. Biol.*, 143 (2003) 14–23.
[28] M. Moghimnezhad, A. Shahidian and M. Andayesh, "Multiphysics Analysis of Ultrasonic Shock Wave Lithotripsy and Side Effects on Surrounding Tissues", *J. Biomed. Phys. Eng.*, 11(6) (2021) 701–712.
[29] M. Mohammadzadeh, J.M. Mercado and C.-D. Ohl, "Bubble Dynamics in Laser Lithotripsy", *J. Phys.*, 656 (2015) 012004.

Table (1) Thermal coefficients for stones treated by Ho:YAG laser

Samples	Stone Type	Wavelength (mm)	$\mu_a(\lambda)$ (mm^{-1})	δ (mm)	τ_{TH} (sec)	$\Delta T(\tau)$ (°C)	t_{st} *10^{-6} (sec)
P1	calcium oxalate	0.3220	3.9658	0.2522	0.0318	1774.94	0.0556
P2	calcium oxalate	0.3194	4.4085	0.2268	0.0257	1411.32	0.0500
P3	calcium oxalate	0.3185	5.0007	0.2000	0.0200	1394.45	0.0441
P4	calcium oxalate	0.3199	4.4377	0.2253	0.0254	1789.83	0.0497
P5	calcium oxalate	0.3182	3.6867	0.2712	0.0368	2837.47	0.0598
P6	calcium oxalate	0.3201	4.8895	0.2045	0.0209	1431.97	0.0451
P7	calcium oxalate	0.3201	4.8895	0.2045	0.0209	2147.96	0.0451
P8	calcium oxalate	0.3201	4.8895	0.2045	0.0209	2147.96	0.0451
P9	uric acid	0.3342	4.9529	0.2019	0.0204	1546.87	0.0582
P10	calcium oxalate	0.3194	4.4085	0.2268	0.0257	1411.32	0.0500
P11	protein	0.3271	3.4492	0.2899	0.0420	1205.45	-
P12	calcium oxalate	0.3208	3.0498	0.3279	0.0538	1977.02	0.0723
P13	calcium oxalate	0.3209	3.0829	0.3244	0.0526	1512.86	0.0715
P14	uric acid	0.3278	4.8432	0.2065	0.0213	2902.03	0.0595
P15	uric acid	0.3278	4.8432	0.2065	0.0213	2321.62	0.0595
P16	calcium oxalate	0.3187	4.1508	0.2409	0.0290	1378.14	0.0531

P17	calcium oxalate	0.3201	4.8895	0.2045	0.0209	2684.94	0.0451
P18	calcium oxalate	0.3308	5.0289	0.1989	0.0198	1574.74	0.0438
P19	uric acid	0.3278	4.8432	0.2065	0.0213	1934.68	0.0595
P20	uric acid	0.3342	4.9529	0.2019	0.0204	1546.87	0.0582
P21	calcium oxalate	0.3194	4.4085	0.2268	0.0257	1411.32	0.0500
P22	calcium oxalate	0.3223	4.9803	0.2008	0.0202	1746.62	0.0443
P23	calcium oxalate	0.3286	5.1006	0.1961	0.0192	2204.47	0.0432
P24	calcium oxalate	0.3201	4.8895	0.2045	0.0209	1431.97	0.0451
P25	uric acid	0.3308	5.8319	0.1715	0.0147	1448.98	0.0494
P26	calcium oxalate	0.3201	4.8895	0.2045	0.0209	1789.96	0.0451
P27	uric acid	0.3333	5.8831	0.1700	0.0144	1799.26	0.0490
P28	calcium oxalate	0.3212	3.7259	0.2684	0.0360	1598.11	0.0592
P29	uric acid	0.3278	4.8432	0.2065	0.0213	1547.75	0.0595
P30	calcium oxalate	0.3201	4.8895	0.2045	0.0209	1431.97	0.0451
P31	calcium oxalate	0.3194	4.4085	0.2268	0.0257	1411.32	0.0500
P32	cystine	0.2752	5.7747	0.1732	0.0150	1736.87	0.0372
P33	calcium oxalate	0.3308	5.0289	0.1989	0.0198	1574.74	0.0438
P34	calcium oxalate	0.3194	4.4085	0.2268	0.0257	1411.32	0.0500
P35	calcium oxalate	0.3201	4.6222	0.2163	0.0234	1069.73	0.0477
P36	uric acid	0.3315	5.4861	0.1823	0.0166	1512.05	0.0525
P37	calcium oxalate	0.3330	6.0347	0.1657	0.0137	1195.11	0.0365
P38	uric acid	0.3333	5.8831	0.1700	0.0144	1799.26	0.0490
P39	calcium oxalate	0.3201	4.8895	0.2045	0.0209	1789.96	0.0451
P40	uric acid	0.3278	4.8432	0.2065	0.0213	1934.68	0.0595

